Supersolid and solitonic phases in the one-dimensional extended Bose-Hubbard model

Tapan Mishra*

Indian Institute of Astrophysics, II Block, Koramangala, Bangalore 560 034, India

Ramesh V. Pai†

Department of Physics, Goa University, Taleigao Plateau, Goa 403 206, India

S. Ramanan‡

Centre for High Energy Physics, Indian Institute of Science, Bangalore 560012, India

Meetu Sethi Luthra§ and B. P. Das‖

Indian Institute of Astrophysics, II Block, Koramangala, Bangalore 560 034, India

We report our findings on the quantum phase transitions in cold bosonic atoms in a one-dimensional optical lattice using the finite-size density-matrix renormalization-group method in the framework of the extended Bose-Hubbard model. We consider wide ranges of values for the filling factors and the nearest-neighbor interactions. At commensurate fillings, we obtain two different types of charge-density wave phases and a Mott insulator phase. However, departure from commensurate fillings yields the exotic supersolid phase where both the crystalline and the superfluid orders coexist. In addition, we obtain the signatures for the solitary waves and the superfluid phase.

I. INTRODUCTION

The supersolid phase, first reported in ^{4}He [1], is characterized by the coexistence of the superfluid and the crystalline orders. While this phase has been predicted in several lattice systems [2–8], there has been no unambiguous observation of this phase so far. Kim and Chan reported its observation in solid ^{4}He [9], but a number of studies disagree with this claim [10–12].

In recent years, the advances in the manipulation of cold bosonic atoms in optical lattices have opened up a new route to investigate quantum phase transitions [13,14]. This approach has many advantages over the conventional solid-state techniques, such as the flexibility in controlling the parameters and the dimension of the lattice by tuning the laser intensity. A system of cold bosonic atoms in an optical lattice can be adequately described by the Bose-Hubbard model [15,16]. However, if the atoms possess long-range interactions due to the presence of magnetic-dipole moments, for example, then they could exhibit a number of different novel phases. In particular, the existence of such interactions could result in the supersolid phase [2,7,17,18]. The fairly recent observation of the Bose-Einstein condensation of ^{52}Cr atoms [19], which have large magnetic-dipole moments, could ultimately lead to the realization of this unusual phase.

*tapan@iiap.res.in

†rvpai@unigoa.ac.in

‡suna@cts.iisc.ernet.in

§Permanent address: Bhaskaracharya College of Applied Sciences, Phase I, Sector 2, Dwarka, Delhi 110075, India; meetu@iiap.res.in

‖das@iiap.res.in

In this context, we reinvestigate the system of bosonic atoms with long-range interaction using the extended Bose-Hubbard model given by

$$H = -t\sum_{\langle i,j\rangle}(a_i^\dagger a_j + \text{H.c.}) + \frac{U}{2}\sum_i n_i(n_i-1) + V\sum_{\langle i,j\rangle} n_i n_j. \quad (1)$$

Here, t is the hopping amplitude between nearest-neighbor sites $\langle i,j\rangle$. $a_i^\dagger(a_i)$ is the bosonic creation (annihilation) operator obeying the bosonic commutation relation $[a_i^\dagger, a_j]=\delta_{i,j}$ and $n_i=a_i^\dagger a_i$ is the number operator. U and V are the on-site and the nearest-neighbor interactions, respectively. We rescale the model Hamiltonian in Eq. (1) in units of the hopping amplitude t by setting $t=1$ and thus making the Hamiltonian and the other quantities dimensionless.

In the absence of any long-range interaction, the model given in Eq. (1) reduces to the Bose-Hubbard model which exhibits a superfluid (SF) to a Mott insulator (MI) transition at integer densities of bosons [15]. However, for noninteger densities, the system remains in the superfluid phase, which is compressible and gapless. The Mott insulator phase, however, has a finite gap and is incompressible. The extended Bose-Hubbard model, given in Eq. (1), has been studied earlier using different methods [2,20–22] including the density matrix renormalization group (DMRG) method [23–25]. The inclusion of the nearest-neighbor interaction gives rise to the charge-density wave (CDW) phase for integer and half-integer densities [2,20–25] that has a finite gap, a finite CDW order parameter, a vanishing compressibility, and a peak in the density structure function at momentum $q=\pi$. In the CDW phase, the bosons occupy alternate sites, the unoccupied ones being empty. For example, when the density $\rho=1/2$, the distribution of bosons has a $|1\ 0\ 1\ 0\ 1\ 0\cdots\rangle$ structure while for $\rho=1$ it is $|2\ 0\ 2\ 0\ 2\ 0\cdots\rangle$. To distin-

guish between these two CDW ground states, the former is referred to as CDW-I and the latter as CDW-II [2]. This model has been studied recently using the quantum Monte Carlo method [2] resulting in the prediction of the supersolid phase when the density of bosons is no longer commensurate. We reinvestigate this model by departing from both half and integer filling for large and intermediate on-site interaction strengths and obtain the phase diagram using the finite-size density-matrix renormalization-group (FS-DMRG) method [26,27] and provide more insights into the supersolid and the solitonic phases.

This paper is organized as follows. In Sec. II, we will discuss the method of our calculation that uses the FS-DMRG method. The results with discussions are presented in Sec. III followed by our conclusions in Sec. IV.

II. METHOD OF CALCULATION

To obtain the ground-state wave function and the energy for a system of N bosons on a lattice of length L, interacting via an on-site and a nearest-neighbor interaction, we use the FS-DMRG method with open boundary conditions [26,27]. This method is best suited for one-dimensional problems and has been widely used to study the Bose-Hubbard model [23–25,27,28]. We have considered four bosonic states per site and the weights of the states neglected in the density matrix formed from the left or the right blocks are less than 10^{-6} [24]. In order to improve the convergence, at the end of each DMRG step, we use the finite-size sweeping procedure given in [24,26]. Using the ground-state wave function $|\psi_{LN}\rangle$ and the corresponding energy $E_L(N)$, we calculate the following physical quantities and use them to identify the different phases. The chemical potential μ of the system having density $\rho=N/L$ is given by

$$\mu = \frac{\delta E_L(N)}{\delta N} \tag{2}$$

and the gaped and the gapless phases are distinguished from the behavior of ρ as a function of μ [29]. The compressibility κ, which is finite for the SF phase, is calculated using the relation

$$\kappa = \frac{\delta \rho}{\delta \mu}. \tag{3}$$

The on-site local number density $\langle n_i \rangle$, defined as,

$$\langle n_i \rangle = \langle \psi_{LN} | n_i | \psi_{LN} \rangle, \tag{4}$$

gives information about the density distribution of different phases and finally the existence of the CDW phase is confirmed by calculating its order parameter

$$O_{\text{CDW}} = \frac{1}{L} \sum_i (-1)^i \langle n_i \rangle. \tag{5}$$

When the ground state is a CDW, the FS-DMRG calculation with open boundary leads to an artificial node in the density distribution at the center due to the reflection symmetry in the algorithm. We circumvent this problem by working with odd number of sites. In our calculations, we start with five sites instead of the usual choice of four sites and increase the length up to L (here, $L=101$) adding two sites in each DMRG iteration [24]. After reaching the desired length L, we vary the number of atoms N from 26 to 125 to scan a wide range of densities [29]. In this work we consider two different values of the on-site interaction strength $U=5$ and 10 and vary the nearest-neighbor interaction strength V from 0 to U. The choice of U is guided by an earlier work [24] where a direct MI to a CDW-II transition for $U=10$ and a MI to a SF to a CDW-II for $U=5$ were observed as V is varied at a density $\rho=1$. In this work, we extend this calculation to a wider range of densities and obtain a richer phase diagram consisting of the supersolid and the solitonic phases in addition to SF, MI, CDW-I, and CDW-II. We begin our discussions for $U=10$ and later comment on our results for $U=5$.

III. RESULTS AND DISCUSSION

It is well known that the Bose-Hubbard model [Eq. (1), with $V=0$] has a superfluid ground state when the density ρ is not an integer and exhibits a quantum phase transition from the superfluid to the Mott insulator phase for integer densities [15] at a critical value of the on-site interaction U_C that depends on ρ. (For example, $U_C \sim 3.4$ for $\rho=1$ [23,24].) The Mott insulator has a finite gap and is incompressible, while the superfluid is gapless and compressible. In the presence of a finite nearest-neighbor interaction V, an additional insulator phase, the CDW, appears at commensurate densities. As noted in [23,24], a CDW-I occurs at $\rho=1/2$ and at $\rho=1$, depending on the value of V either a MI or a CDW-II appears. Since we are dealing with only an on-site and a nearest-neighbor interaction, the commensurate densities for the model in Eq. (1) are integers and half integers. We begin by studying the possible phases at commensurate densities before we investigate the phases at incommensurate densities.

The gaped phases are easily obtained from the dependence of the density ρ and the compressibility κ on the chemical potential μ. Figure 1 shows the dependence of ρ on μ for a fixed value of $U=10$ and V ranging between 2 and 10. The gaped phases appear as plateaus with the gap equal to the width of the plateau, i.e., $\mu^+ - \mu^-$, where μ^+ and μ^- are the values of the chemical potential at the upper knee and the lower knee of the plateau, respectively. For small values of V, Fig. 1 has only one plateau at $\rho=1$. However, as we increase V, an additional plateau appears at $\rho=1/2$. We calculate the compressibility using Eq. (3) and is also given as a function of μ in Fig. 2 for two generic values of V. The smaller value, $V=2$, has just one plateau at $\rho=1$, while $V=7$ has two, at densities $\rho=1/2$ and 1. As expected, the compressibility is zero over the range of μ values where the plateaus occur, while it is finite elsewhere. The incompressible insulator and the compressible superfluid regions can be separated out by picking up μ^+ and μ^- and plotting them in the $\mu-V$ plane. From Figs. 1 and 2, we see that (i) a gaped phase occurs at $\rho=1/2$ for $V \gtrsim 2.8$, (ii) for $\rho=1$, the gap remains finite for all values of V, and (iii) the gap is zero for other values of ρ.
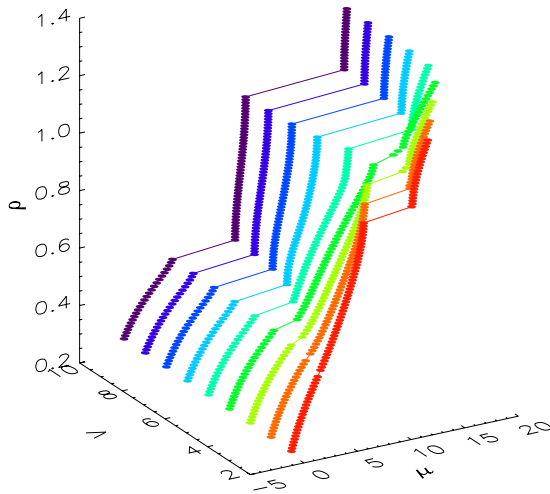
FIG. 1. (Color online) The density ρ as a function of the chemical potential μ for different values of V. The plateaus at commensurate fillings indicate the existence of a finite gap in the system.

The nature of the compressible and the incompressible phases can be further understood from the local-density distribution $\langle n_i \rangle$ and the charge-density wave order parameter O_{CDW} given by Eqs. (4) and (5), respectively. The variation of the local density as a function of the lattice sites is given in Figs. 3 and 6 for densities around $\rho = 1/2$ and 1, respectively. At commensurate densities, say, $\rho = 1/2$, the charge-density wave nature of the phase is clearly observed for $V = 5.6$ in Fig. 3(c). An alternate variation of the density of bosons between one and zero, i.e., $|1 \ 0 \ 1 \ 0 \ 1 \ 0 \cdots\rangle$, is the signature of the CDW-I phase [2,23]. Similarly, for $\rho = 1$, the density oscillations of the type $|2 \ 0 \ 2 \ 0 \ 2 \ 0 \cdots\rangle$ for $V = 9$ suggest the CDW-II phase. From the gap, the compressibility, and the density oscillations, we can conclude that for $U = 10$ and $\rho = 1/2$, we have a SF to a CDW-I phase transition at $V \sim 2.8$. However, for $\rho = 1$, there is no superfluid phase and the transition is from a MI to a CDW-II at a critical value $V_C \sim 5.4$. These results are consistent with the earlier ones in the literature [2,23,24].
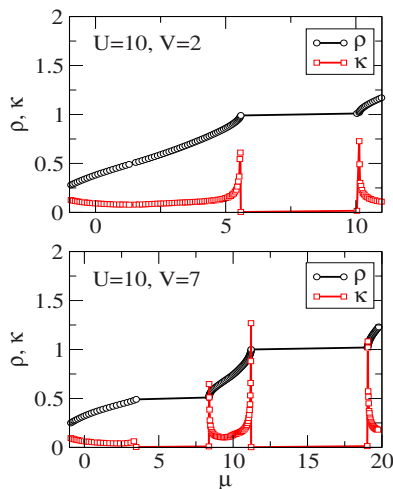

FIG. 2. (Color online) Variation of κ and ρ with μ for $V = 2$ (top panel) and $V = 7$ (bottom panel). The plateau regions have zero compressibility while it is finite elsewhere.
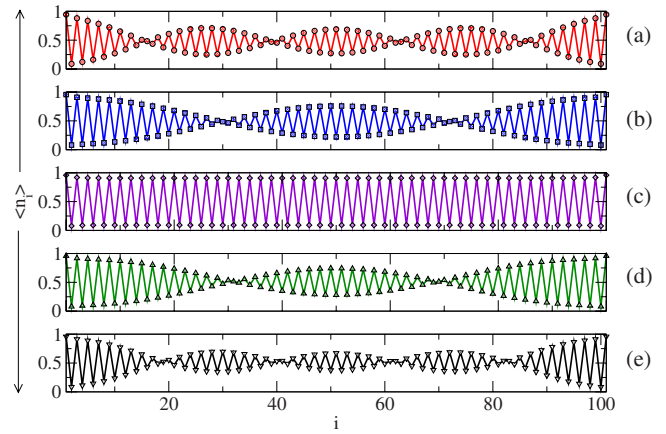

FIG. 3. (Color online) Local density $\langle n_i \rangle$ as a function of lattice sites i. Panels (a) and (b) show the solitonic signature when $\rho < 1/2$. (c) shows the signature of the CDW-I phase where every alternate site is occupied by one boson for $\rho = 1/2$. Panels (d) and (e) show the modulation of the CDW-I phase for $\rho > 1/2$ and are once again in the solitonic phase.

We now turn our attention to the case when ρ is not commensurate to the lattice length, i.e., $\rho \neq 1/2$ or 1. From Fig. 2, we observe that the compressibility is always finite for incommensurate densities indicating that these regions of the phase diagram correspond to the superfluid phase. However, the local-density distribution and the CDW order parameter, O_{CDW}, reveal the richness of the phases present in the compressible regions of the phase diagram. Interesting phases appear when the nearest-neighbor interaction is large enough to obtain a CDW-I or a CDW-II phase at commensurate densities. Let us first consider densities close to $\rho = 1/2$. When V is less than the critical value $V_C \sim 2.8$ for the SF-CDW transition, we expect only the superfluid phase. However, for $V > V_C$, the ground state shows a solitonic behavior for densities close to $\rho = 1/2$. Figure 3 shows the local densities $\langle n_i \rangle$ as a function of the lattice sites i for small departures from the commensurate filling value. The panel labeled (c) corresponds to the commensurate density $\rho = 1/2$ where we clearly observe the CDW nature of the ground state, (b) and (d), respectively, show the density variations of the ground state when one boson has been added and removed from the system at $\rho = 1/2$. Similarly, panels (a) and (e), respectively, show the density variations when two bosons have been added and removed. The density profiles can be understood as follows. Moving away from commensurate densities, the solitons distort the periodic ground state by breaking the long-range crystalline order as a modulation in the density wave that minimizes the ground-state energy of the system [2,30].

To understand the solitons, we calculate the CDW order parameter for each unit cell. In contrast to the superfluid and the Mott insulator phases that have one site per unit cell, the CDW phase consists of two lattice sites per cell. Referring to these two sites as 1 and 2, we define the CDW order parameter per unit cell as

$$O_{CDW}^{cell} = \langle n_1 \rangle - \langle n_2 \rangle. \qquad (6)$$

The CDW phase has two degenerate ground states corresponding to the two local-density distributions
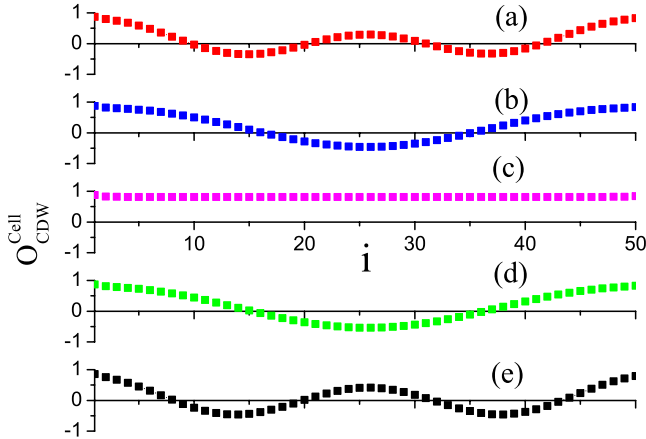
FIG. 4. (Color online) CDW order parameter per unit cell O_{CDW}^{cell} as a function of sites. (a) and (b) exhibit the solitonic signature for densities $\rho < 1/2$. In panel (c), O_{CDW}^{cell} is flat, thereby indicating CDW-I with alternate sites occupied by one boson. (d) and (e) show the signature for the solitons at densities $\rho > 1/2$.

$|1\ 0\ 1\ 0\ 1\ 0\cdots\rangle$ and $|0\ 1\ 0\ 1\ 0\ 1\cdots\rangle$. The CDW order parameter, O_{CDW}^{cell}, for these two degenerate states equals 1 and -1, respectively. Figure 4 shows the O_{CDW}^{cell} for the same set of densities considered in Fig. 3. In Fig. 4, the center panel (c) has density $\rho = 1/2$, while (b) and (d) represent the case where one boson has been added and removed, respectively, from the system in panel (c) and (a) and (e) have two bosons added and removed with respect to (c). We notice that the O_{CDW}^{cell} is uniform and close to one for $\rho = 1/2$. Since we work with odd number of sites with open boundaries, energy considerations lead to a CDW ground state $|1\ 0\ 1\ 0\ 1\ 0\cdots\rangle$. When we add or remove one boson from this state, we get two solitons that modulate the density distribution and break the long-range crystalline order. The extra particle or hole splits into two solitons of equal mass [30,31]. The two solitons can move across the lattice without causing any energy, however, if we want to get rid of them, we need to spend lots of energy to flip the bosons.

Similarly, the removal or the addition of two bosons results in four solitons. The number of solitons increases as the bosons are further added or removed, until a critical density is reached, when the density oscillation completely dies out and a superfluid phase is obtained. Therefore, starting with the CDW-I phase and changing the density from its commensurate value of $\rho = 1/2$ by either adding or removing bosons leads to the solitons+SF phase that finally becomes a superfluid. The transition from the solitonic to the superfluid phase is more like a *crossover* than a real phase transition. The solitonic phase is obtained only very close to $\rho = 1/2$ and remains stable for the entire range of V considered on the hole side ($\rho < 1/2$). However, on the particle side ($\rho > 1/2$), the solitonic phase remains stable only up to some critical value of $V = V_C \sim 6.4$. For $V > 6.4$, doping below half filling breaks the CDW ground state into a solitonic state that eventually goes into a superfluid phase. However, this does not happen when bosons are added above half filling. For example, the variation of $\langle n_i \rangle$ as a function of the lattice sites i for three different densities are given in Fig. 5 for $V = 9$. The
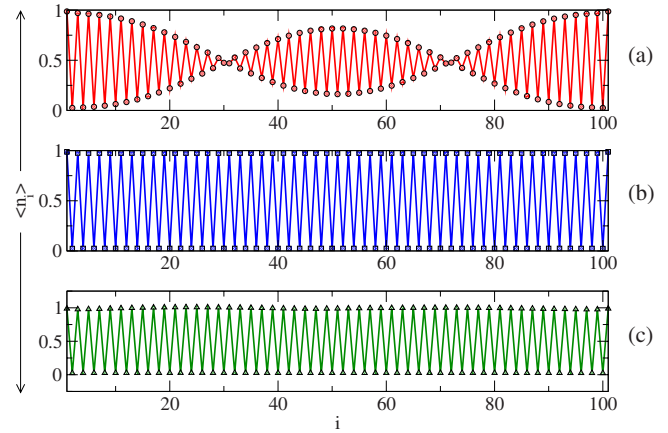

FIG. 5. (Color online) Variation of the local density $\langle n_i \rangle$ as a function of i for $V = 9$. Panel (a) shows the ground-state density when a boson is removed from the state at $\rho = 1/2$ shown in panel (b) that is in a CDW-I phase and panel (c) corresponds to the state obtained by adding a boson to $\rho = 1/2$ state.

panel (b) represents the CDW-I phase at $\rho = 1/2$ while (a) and (c) correspond to the ground state obtained by removing and adding one boson, respectively, to the CDW-I ground state. A solitonic phase appears when the bosons are removed (i.e., for $\rho < 1/2$), however, Fig. 5(c) suggests that the CDW-I phase is robust for $\rho > 1/2$. Similar behavior is also seen when doping around $\rho = 1$. Figure 6 shows $\langle n_i \rangle$ as a function of i for densities around $\rho = 1$. Panels (a) and (c) correspond to the density of the ground state obtained by removing and adding one boson to the CDW-II state [panel (b)] at a density $\rho = 1$.

It turns out that for large V, the region between $1/2 < \rho < 1$, i.e., between the CDW-I and the CDW-II, always remains in the crystalline phase even though the density is not commensurate to the lattice length. The CDW order in the system is determined by calculating the CDW order parameter using Eq. (5) and is given in Fig. 7. For small values of
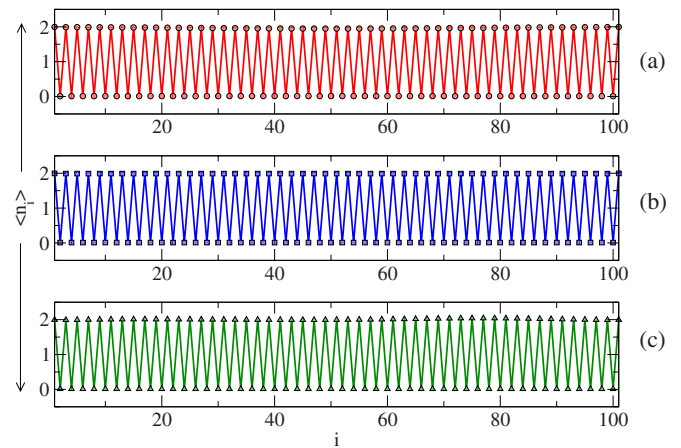

FIG. 6. (Color online) Variation of the local density as a function of the lattice sites i for doping around $\rho = 1$ for $V = 9$. Panel (b) corresponds to the CDW-II phase at $\rho = 1$ and panels (a) and (c) to the state obtained by removing and adding a boson to the CDW-II state. Notice that the crystalline structure is preserved for these density changes.
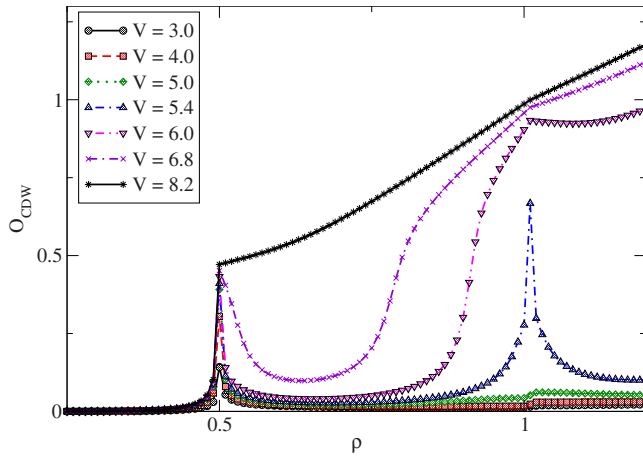
FIG. 7. (Color online) O_{CDW} as a function ρ for different V. The two peaks at commensurate densities show the existence of CDW-I and the CDW-II phases. The finite order parameter for large values of V in the incommensurate density range shows the signature of the supersolid phase.
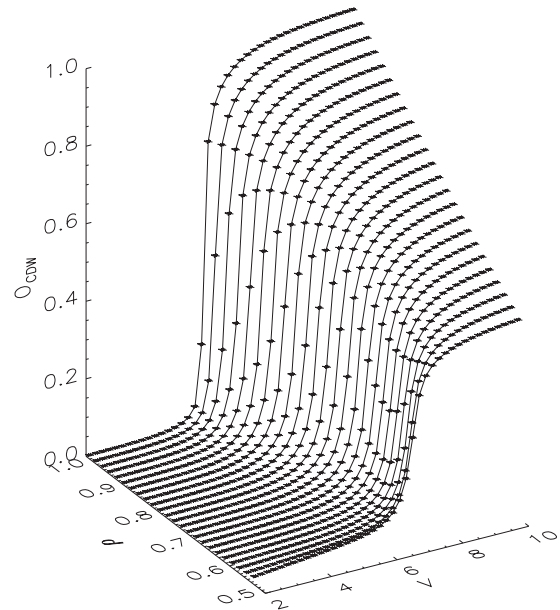

FIG. 8. The CDW order parameter O_{CDW} as a function of V for different densities in the range $1/2 \leq \rho \leq 1$. Note that O_{CDW} increases as V increases.

V, O_{CDW} is zero for all densities except at $\rho = 1/2$ signaling the CDW-I phase. However, as V increases, an additional peak develops at $\rho = 1$ for $V > 5.4$ corresponding to the CDW-II phase. The most interesting feature is that O_{CDW} remains finite in the region $1/2 < \rho < 1$ for large values of V. It may be noted that the compressibility for $1/2 < \rho < 1$ is always finite. So the bosons move freely on the CDW background and prefer to occupy sites that are already filled. Consider the case when a boson is added to the CDW-I ground state, which has $\rho = 1/2$. If the added boson occupies an empty site, the energy cost is only due to the nearest-neighbor interaction and is of the order of $2V$. However, if the added boson occupies a site that is already filled, the energy cost is due to the on-site interaction and is of the order of U, which is relatively small compared to $2V$ for large V. The extra bosons therefore move between the occupied sites with a finite hopping amplitude leading to a long-range correlation in the lattice, resulting in a compressible region for the range of densities $1/2 < \rho < 1$ as shown in Fig. 2. Similar behavior persists for doping above $\rho = 1$ as given in Fig. 6.

Therefore we can conclude that for small V values apart from commensurate fillings, there exists no finite CDW order that is gapless and incompressible. But for large V value, the CDW order remains finite for incommensurate densities. As a result, the region in the phase diagram between the CDW-I and the CDW-II exhibits the coexistence of both the diagonal long-range order (DLRO) and the off-diagonal long-range order (ODLRO) that is the signature of the supersolid. In order to obtain the boundary that separates the supersolid phase in the phase diagram, we plot O_{CDW} with respect to V for different densities as given in Fig. 8. We note that O_{CDW} increases sharply at some critical value of V, highlighting the transition to the CDW phase. To obtain this critical value of V, we take the derivatives of O_{CDW} with respect to V for different densities in the range $1/2 < \rho < 1$ and $\rho > 1$. The point where the derivative is a maximum is taken to be the critical point of the transition to the CDW phase. The order

parameter O_{CDW}, as well as its derivative as a function of V, is shown in Fig. 9. The derivative shows a negligible peak for $\rho < 1/2$, but it shows a sharp peak for $\rho > 1/2$ indicating the existence of the CDW phase.

The phase diagram, obtained by plotting the chemical potential μ corresponding to different densities as a function of V, is given in Fig. 10. To identify the region where the gaped phases exist, we calculate the chemical potentials μ^+ and μ^- [25,29] at $\rho = 1/2$ and 1 for all values of V in the thermodynamic limit and plot them in the $\mu - V$ plane. The boundary of the supersolid phase is obtained by calculating the chemical potential μ for $0.5 < \rho < 1$ and $\rho > 1$ at the critical value of V where the system enters into the CDW phase. The critical value of V for the transition to the supersolid phase (SS)
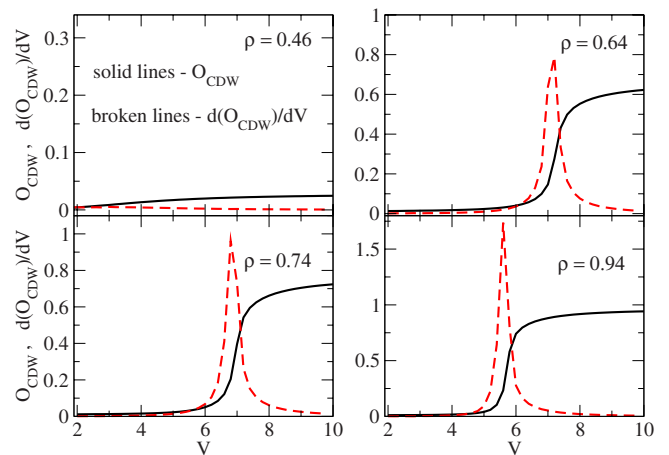

FIG. 9. (Color online) CDW order parameter O_{CDW} (solid lines) and its derivative with respect to V (broken lines). For $V \geq V_C \sim 6.4$, the derivative exhibits a peak at the transition to the CDW phase.
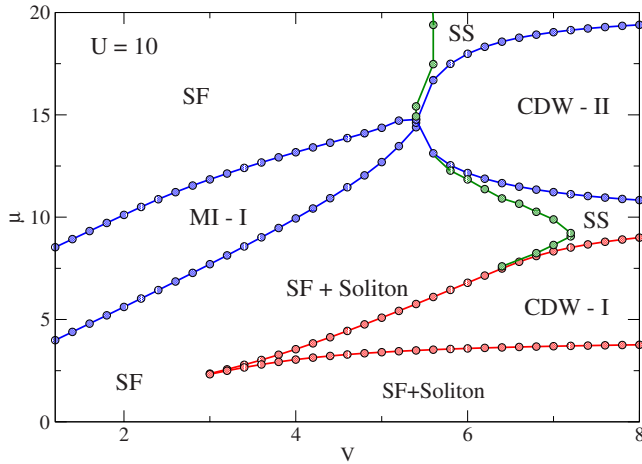
FIG. 10. (Color online) Phase diagram showing all the phases for $U=10$.

FIG. 11. (Color online) Phase diagram showing all the phases for $U=5$.

for densities close to $\rho=0.5$ is $V_C \sim 6.4$. This critical value depends on the density of bosons, exhibiting an increase as the system is further doped and has a minimum value of $V_C=5.4$. For large values of V, it is clearly seen that the system continues to be in the supersolid phase above CDW-II, while for smaller values of V, it is in the SF phase.

The results remain qualitatively similar when $U=5$ and the corresponding phase diagram is given in Fig. 11. In this case, the gaped regions such as CDW-I, CDW-II, and MI shrink. There is no direct transition from MI to CDW-II in sharp contrast to $U=10$. Rather, there are continuous MI-SF and SF-CDW-II transitions. The supersolid phase occurs in a small region close to $\rho \lesssim 1$, but the trend is similar to that of $U=10$ for $\rho>1$. For low values of U, the gap in the CDW phase is very small and the hopping element plays a dominant role in minimizing the energy of the system. Therefore, when the density of the system is moved away from the commensurate value, the CDW phase is easily destroyed. This leads to drastic reduction of the supersolid region compare to large U case.

IV. CONCLUSIONS

In summary, we have obtained the complete phase diagram for single species bosonic atoms in the framework of the extended Bose-Hubbard model for two different values of the on-site interaction U. Our studies have been carried out using the FS-DMRG method for a large range of densities: $0.25 \leq \rho \leq 1.25$. In the large U limit, we obtain the
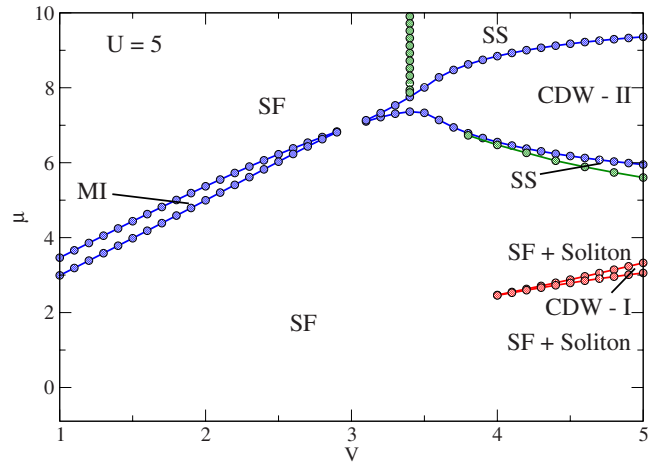
CDW-I, the MI, the CDW-II, the SF, the soliton, and the supersolid phases, the transitions between them occurring at various critical values of the nearest-neighbor interaction. The supersolid phase appears in the density range $0.5 < \rho < 1$ and $\rho > 1$ only in the large V regime. The solitons are found to exist for doping above half filling in the small V regime and for doping below half filling for the entire range of V. For an on-site interaction of intermediate strength ($U=5$), we find an interesting change in the phase diagram. The supersolid phase becomes very small in the density range $0.5 < \rho < 1$ and it exists only at densities close to 1.

From an experimental point of view, in addition to the optical lattice, there is always a magnetic trap present, thereby making these systems inhomogeneous. Therefore, it makes it imperative to study this model in the presence of a harmonic trap, where all the phases coexist. There have been several experiments as well as theoretical predictions of the different quantum phases using dipolar atoms in the recent years [32–36]. Hence, it becomes important to look for the experimental signatures of these phases in the presence of a trap in order to make reliable predictions and this is currently in progress.

[1] O. Penrose and L. Onsager, Phys. Rev. **104**, 576 (1956).

[2] G. G. Batrouni, F. Hebert, and R. T. Scalettar, Phys. Rev. Lett. **97**, 087209 (2006).

[3] D. Heidarian and K. Damle, Phys. Rev. Lett. **95**, 127206 (2005).

[4] R. G. Melko, A. Paramekanti, A. A. Burkov, A. Vishwanath, D. N. Sheng, and L. Balents, Phys. Rev. Lett. **95**, 127207 (2005).

[5] P. Sengupta, L. P. Pryadko, F. Alet, M. Troyer, and G. Schmid, Phys. Rev. Lett. **94**, 207202 (2005).

[6] S. Wessel and M. Troyer, Phys. Rev. Lett. **95**, 127205 (2005).

[7] V. W. Scarola, E. Demler, and S. Das Sarma, Phys. Rev. A **73**,

051601(R) (2006).

[8] P. P. Orth, D. L. Bergman, and K. Le Hur, Phys. Rev. A **80**, 023624 (2009).

[9] E. Kim and M. H. W. Chan, Nature (London) **427**, 225 (2004); Science **305**, 1941 (2004).

[10] Ann Sophie C. Rittner and J. D. Reppy, Phys. Rev. Lett. **97**, 165301 (2006).

[11] S. Sasaki, R. Ishiguro, F. Caupin, H. Maris, and S. Balibar, Science **313**, 1098 (2006).

[12] L. Pollet, M. Boninsegni, A. B. Kuklov, N. V. Prokofev, B. V. Svistunov, and M. Troyer, Phys. Rev. Lett. **98**, 135301 (2007).

[13] M. Greiner, O. Mandel, T. Esslinger, T. W. Haensch, and I. Bloch, Nature (London) **415**, 39 (2002).

[14] I. Bloch, J. Dalibard, and W. Zwerger, Rev. Mod. Phys. **80**, 885 (2008).

[15] M. P. A. Fisher, P. B. Weichman, G. Grinstein, and D. S. Fisher, Phys. Rev. B **40**, 546 (1989).

[16] D. Jaksch, C. Bruder, J. I. Cirac, C. W. Gardiner, and P. Zoller, Phys. Rev. Lett. **81**, 3108 (1998).

[17] T. Mishra, R. V. Pai, and B. P. Das, e-print arXiv:0906.2551.

[18] L. Mathey, Phys. Rev. B **75**, 144510 (2007).

[19] A. Griesmaier, J. Werner, S. Hensler, J. Stuhler, and T. Pfau, Phys. Rev. Lett. **94**, 160401 (2005).

[20] V. A. Kashurnikov and B. V. Svistunov, Phys. Rev. B **53**, 11776 (1996).

[21] G. G. Batrouni, R. T. Scalettar, G. T. Zimanyi, and A. P. Kampf, Phys. Rev. Lett. **74**, 2527 (1995).

[22] P. Niyaz, R. T. Scalettar, C. Y. Fong, and G. G. Batrouni, Phys.

[23] T. D. Kuhner and H. Monien, Phys. Rev. B **58**, R14741 (1998).

[24] R. V. Pai and R. Pandit, Phys. Rev. B **71**, 104508 (2005).

[25] T. D. Kuhner, S. R. White, and H. Monien, Phys. Rev. B **61**, 12474 (2000).

[26] S. R. White, Phys. Rev. Lett. **69**, 2863 (1992); Phys. Rev. B **48**, 10345 (1993).

[27] U. Schollwöck, Rev. Mod. Phys. **77**, 259 (2005).

[28] L. Urba *et al.*, J. Phys B **39**, 5187 (2006).

[29] S. Ramanan, T. Mishra, M. S. Luthra, R. V. Pai, and B. P. Das, Phys. Rev. A **79**, 013625 (2009).

[30] F. J. Burnell, M. M. Parish, N. R. Cooper, and S. L. Sondhi, e-print arXiv:0901.4366.

[31] M. Kumar, S. Sarkar, and S. Ramasesha, e-print arXiv:0812.5059.

[32] J. Stuhler, A. Griesmaier, T. Koch, M. Fattori, T. Pfau, S. Giovanazzi, P. Pedri, and L. Santos, Phys. Rev. Lett. **95**, 150406 (2005).

[33] T. Lahaye, T. Koch, B. Fröhlich, M. Fattori, J. Metz, A. Griesmaier, S. Giovanazzi, and T. Pfau, Nature (London) **448**, 672 (2007).

[34] C.-M. Chang, W.-C. Shen, C.-Y. Lai, P. Chen, and D.-W. Wang, Phys. Rev. A **79**, 053630 (2009).

[35] A. Polkovnikov, E. Altman, and E. Demler, Proc. Natl. Acad. Sci. U.S.A. **103**, 6125 (2006).

[36] V. Gritsev, E. Altman, E. Demler, and A. Polkovnikov, Nat. Phys. **2**, 705 (2006).